

Supplementary document

Role of Iron Contaminants in the Pathway of Ultra-Stable Y Zeolite Degradation

Qianqian Liu^a, Bo Peng^a, Qiaoqiao Zhou^b, Aiguo Zheng^a, Xiuzhi Gao^a, Yu Qi^b, Shuai
Yuan, Yuxia Zhu^a, Lian Zhang^b, Haitao Song^{a*} and Zhijian Da^{a*}

^a Research Institute of Petroleum Processing, SINOPEC, Beijing, 100083, China

^b Department of Chemical & Biological Engineering, Monash University,
Wellington Road, Clayton, Victoria 3800, Australia

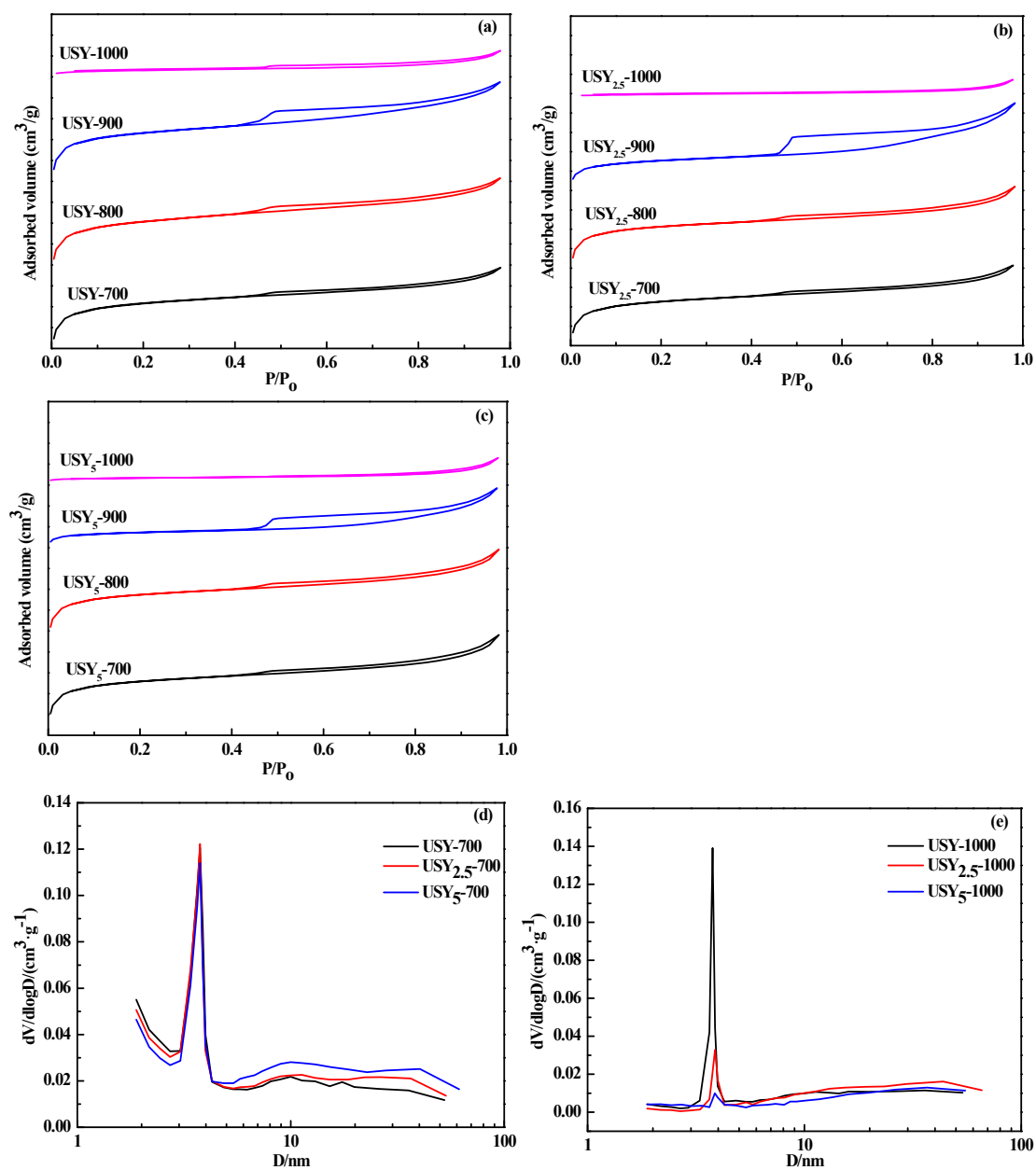


Fig. S1 N₂ adsorption-desorption isotherms and pore size distribution curves for

parent and iron contaminated USY zeolite after calcination

(a)-(c) N₂ adsorption-desorption isotherms for USY, USY_{2.5}, USY₅ calcinated at 700 °C,

800 °C, 900 °C, 1000 °C; (d)-(e) pore size distribution curves for USY, USY_{2.5}, USY₅

calcinated at 700 °C and 1000 °C

The N₂ adsorption-desorption isotherms and pore size distribution curves for

parent and iron contaminated USY zeolite after calcination are given in Fig. S1. The

hysteresis loop in the adsorption–desorption isotherms is ascribed to capillary condensation effects and reveals the presence of mesopores. At higher relative pressures ($P/P_0 > 0.8$) the adsorption and desorption branches of the isotherm are nearly parallel, suggesting that the mesopores are mainly open and channel-like. However, the sudden closure of the hysteresis loop at $P/P_0 = 0.45$ points to cavitation resulting from the presence of blocked mesopores that can only be accessed either through micropores (“closed” mesopores) or through openings with a diameter of less than 4 nm (constricted mesopores).¹

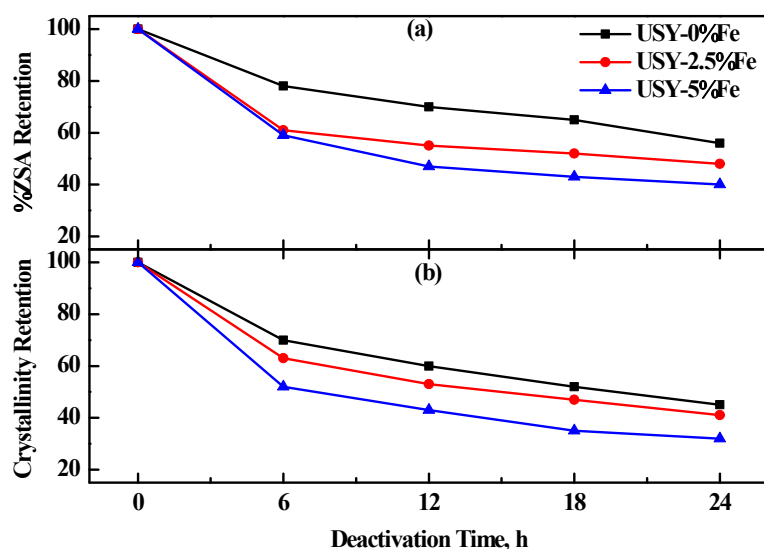


Fig. S2 Hydrothermal stability of parent and iron contaminated USY zeolite

Table S1 Ethylcyclohexane cracking over parent and iron contaminated USY zeolite

before and after thermal treatment						
	USY	USY _{2.5}	USY ₅	USY-900	USY _{2.5} -900	USY ₅ -900
Reaction temperature/°C	500					
$Sv^{-1}/g \cdot h \cdot mol^{-1}$						
Conversion/%	28.73	28.45	28.52	18.54	10.51	6.62
Hydrogen	0.06	0.23	0.35	0.04	0.12	0.19
Methane	0.69	0.52	0.41	0.61	0.15	0.12
Ethane	1.21	1.18	1.16	1.11	0.33	0.27

	Ethylene	2.26	2.52	2.86	2.10	0.44	0.39
Dry gas		4.23	4.45	4.78	3.86	1.03	0.97
	Propane	1.75	1.53	1.44	0.72	0.55	0.22
	Propylene	5.50	5.48	5.33	3.67	1.50	0.88
	n-Butane	1.79	1.72	1.66	0.70	0.65	0.22
	Isobutane	1.63	1.68	1.66	0.55	0.55	0.14
	1-Butene	1.47	1.49	1.51	0.95	0.47	0.25
	Isobutylene	1.92	1.93	1.92	1.03	0.65	0.30
	c-2-Butene	1.22	1.21	1.23	0.76	0.43	0.22
	t-2-Butene	1.59	1.41	1.52	0.99	0.57	0.29
	Butadiene	0.02	0.02	0.02	0.02	0.00	0.00
LPG		16.90	16.47	16.29	9.38	5.37	2.54
Liquid yield		7.48	7.36	7.25	5.25	4.03	3.08
Coke		0.13	0.17	0.20	0.05	0.08	0.03

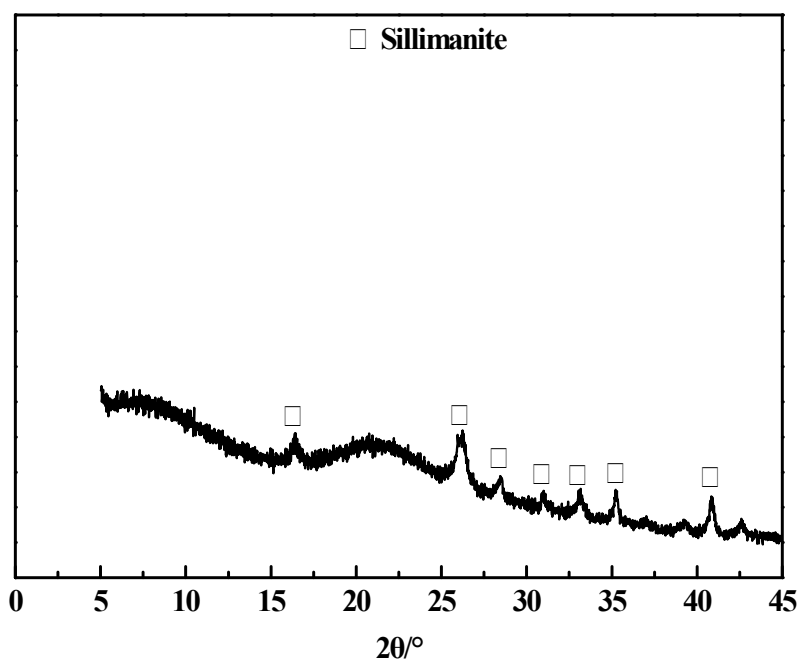


Fig. S3 XRD patterns of USY after calcination at 1100 °C for 2h

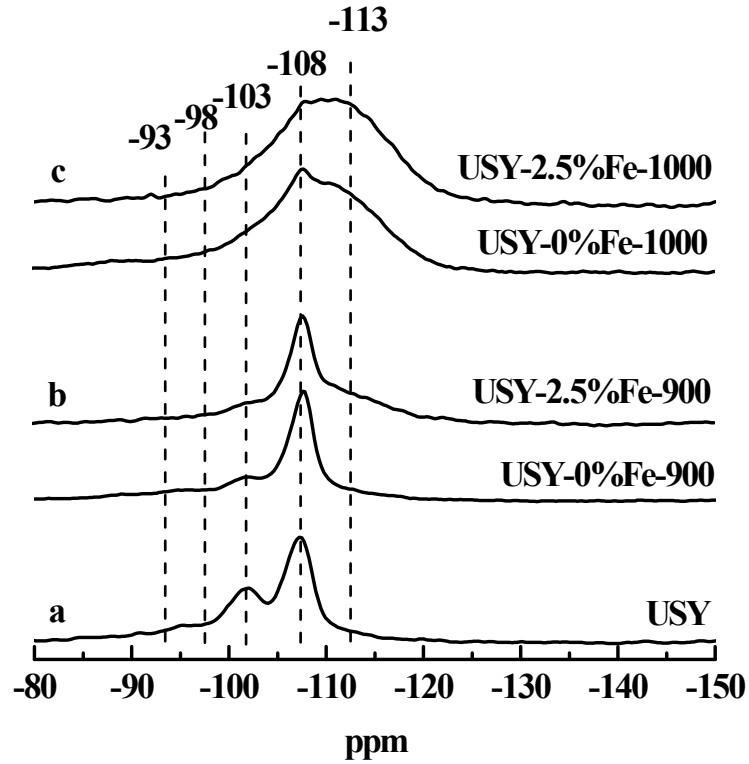
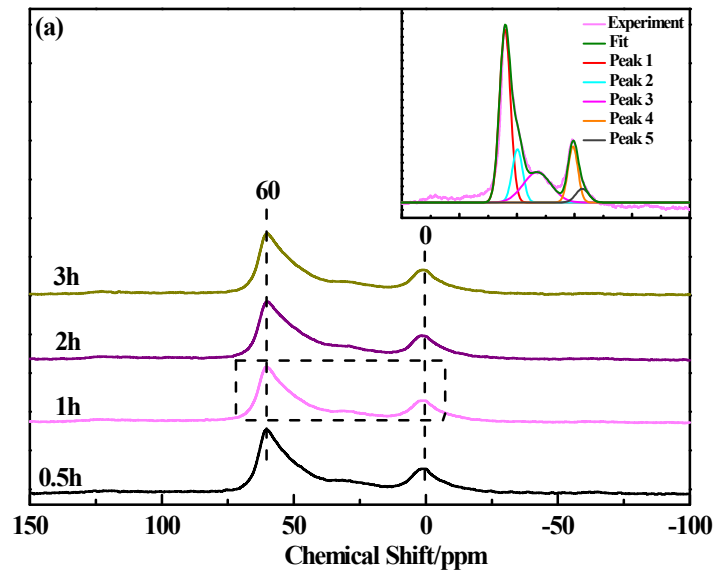


Fig. S4 ^{29}Si -NMR of parent and iron contaminated USY zeolite after calcinated at different temperature



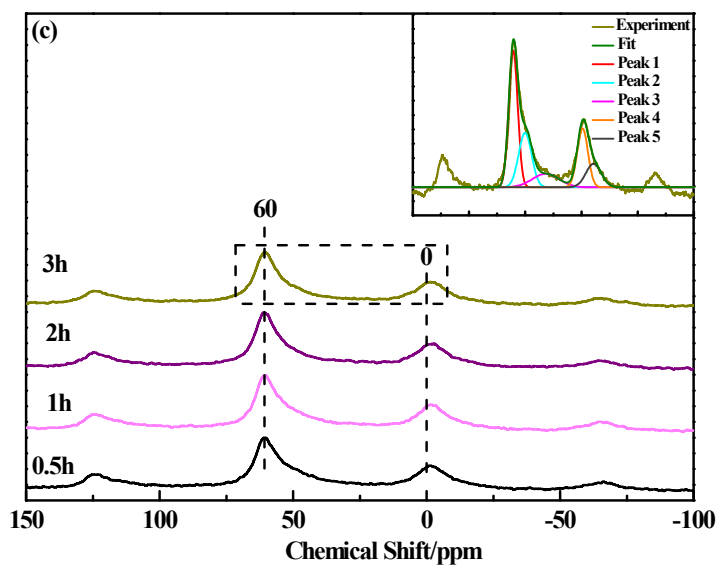
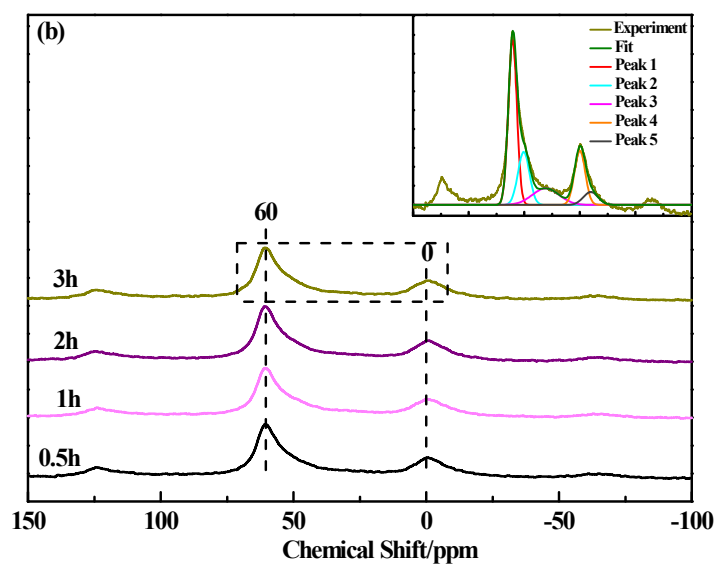


Fig. S5 Al^{27} -NMR of parent and iron contaminated USY zeolite after calcination at 800

°C for different time

(a) USY-0; (b) USY-2.5%Fe; (c) USY-5%Fe

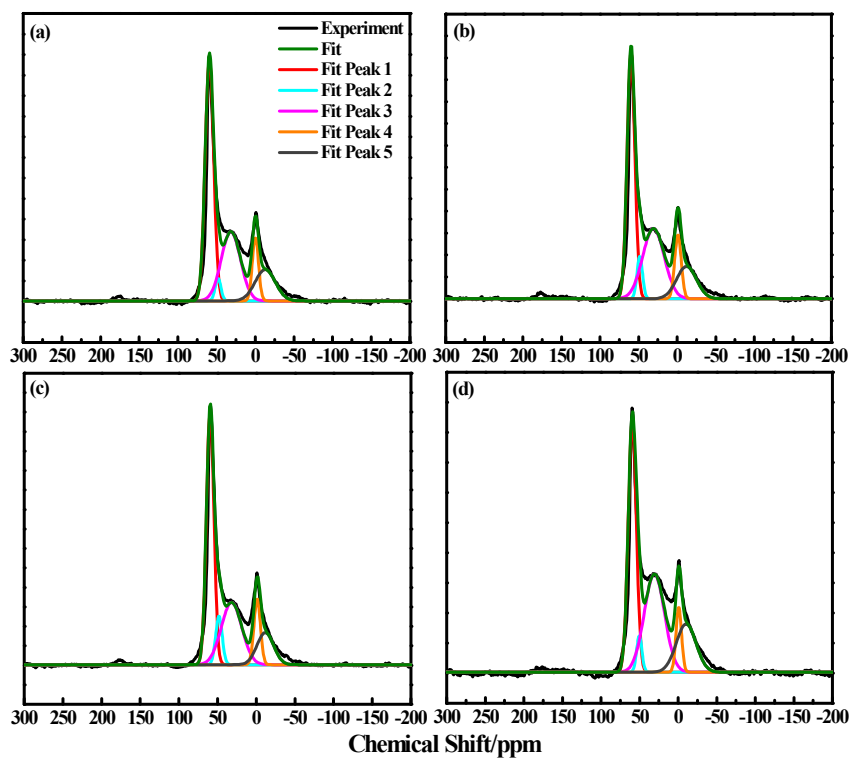


Fig. S6 Al^{27} -NMR and fitting results of parent USY zeolite after calcination at $900\text{ }^\circ\text{C}$

for different time

(a) 0.5h; (b) 1h; (c) 1.5h; (d) 2h

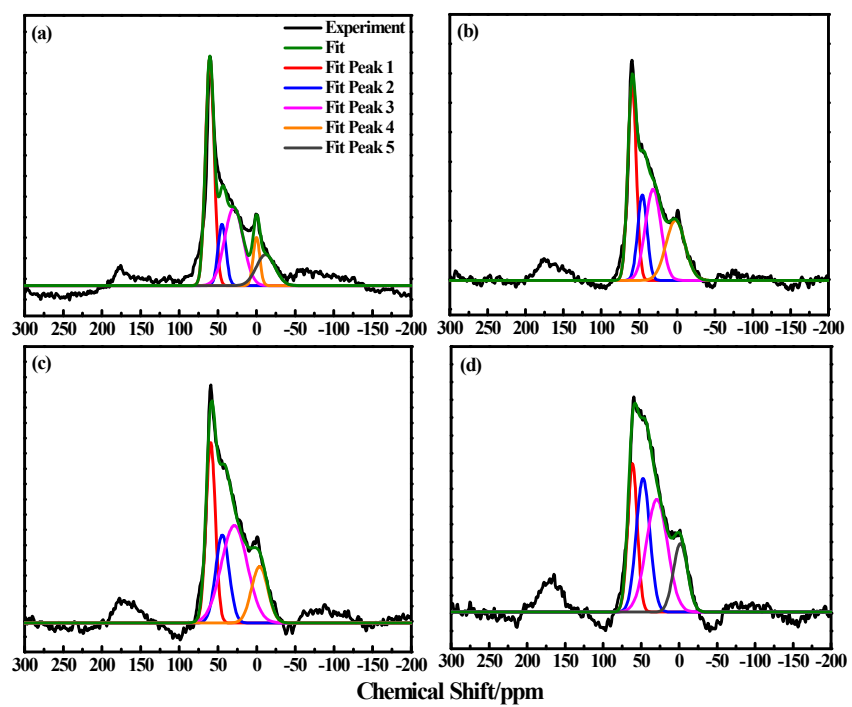


Fig. S7 Al^{27} -NMR and fitting results of USY-2.5%Fe after calcination at $900\text{ }^\circ\text{C}$ for

different time

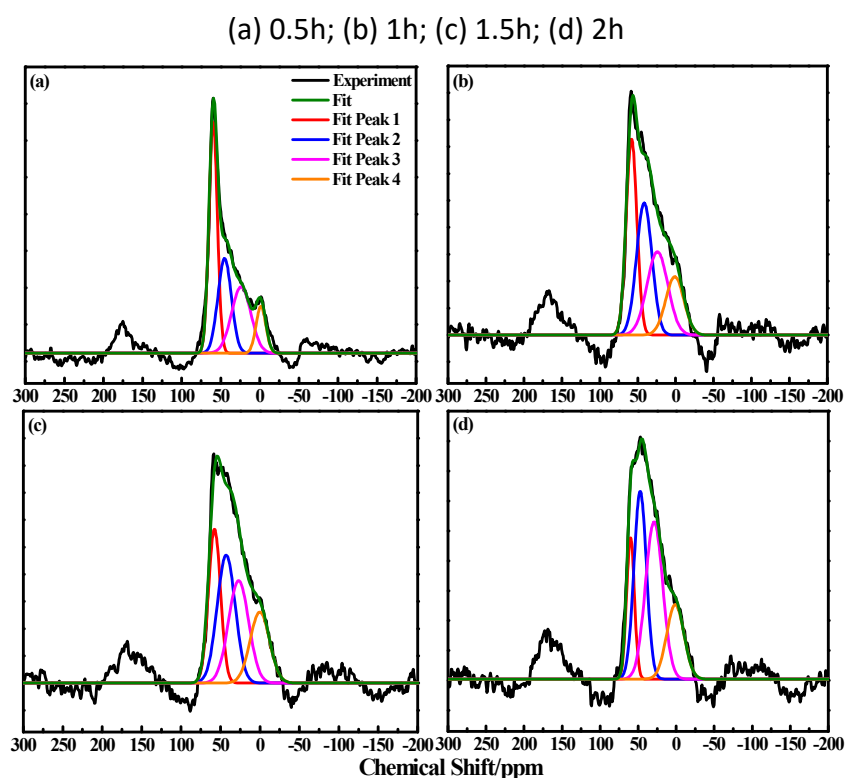


Fig. S8 Al^{27} -NMR and fitting results of USY-5%Fe after calcination at 900 °C for different time

(a) 0.5h; (b) 1h; (c) 1.5h; (d) 2h

Fig. S9 The elemental distribution of USY_5 calcinated at 1000 °C by STEM

Table S2 Main parameters used in EXAFS fitting for $\text{USY}_{2.5}$ calcinated at different temperatures

	R-range	K-range
$\text{USY}_{2.5}$ -800	1-3.6	0.5-6.2
$\text{USY}_{2.5}$ -900	1-3.1	0.5-7
$\text{USY}_{2.5}$ -1000	1-3.1	0.5-7